Open-Loop Power Adaptation in Nanosensor Networks for Chemical Reactors

Eisa Zarepour, Mahbub Hassan, Chun Tung Chou, and Adesoji A. Adesina

***Abstract*—Due to their extremely small form factor, wireless nanosensor networks (WNSNs) have the potential to monitor and control chemical processes right at the molecule level lifting the process efficiency to a level not possible with conventional methods. However, sensor networking within a chemical reactor is challenging due to its time-varying chemical composition, which creates a time-varying radio channel. The nanosensors therefore need to continuously adapt their transmission power according to the chemical composition while maintaining a low overall power budget. We show that this problem can be modeled as a Markov decision process (MDP). However, the MDP solution requires the sensors to know the composition of the reactor at each time instance, which is difficult to realize due to computation and communication constraints at the nanoscale. We therefore choose to use open-loop methods for power adaptation, which allows nanosensors to dynamically adjust their powers based on a policy derived entirely from offline analysis of the expected channel variation over time. Using extensive simulations, we evaluate the performance of the proposed open-loop power adaptation method for improving the efficiency of a widely deployed gas-to-liquid conversion process known as Fischer-Tropsch (FT) synthesis. We find that the proposed method performs close to optimal achieving a three fold improvement in FT efficiency with only a 100 femto watt power consumption on average for the nanosensor communications. In terms of maximum achievable process efficiency, our method outperforms the previously proposed open-loop power adaptation policy by 30% and the nonadaptive power allocation by 52%.**

***Index Terms*—Controlling chemical reactors, MDP, open loop power allocation, power optimization/adaptation, wireless nanoscale sensor networks, wireless sensor networks, WNSNs for chemical catalysis.**

I. Introduction

NANOSENSORS are tiny motes (nanomotes) made from novel nanomaterials capable of sensing new types of phenomenon at the molecular level. For example, a hydrogen nanosensor was reported in [33], where the optical properties of the palladium layer changes when exposed to hydrogen. Yonzon et al. [39] survey many other types of nanosensors that can be used for chemical and biological sensing. Similarly, significant progress has been made in building nanoactuators that can be used to accomplish some basic tasks at the molecular level by harnessing the interactions between nanoparticles, electromagnetic fields and heat [3], [9]. The next step is to connect these nanosensors into a wireless nano sensor network (WNSN) for wider coverage and control of the environment. WNSNs open up the possibility to sense and control important physical processes from the very *bottom*, right at the molecule level. There are early indications suggesting that such *bottom-up* approach to sensing and control, which has hitherto not been possible with conventional macro-scale wireless sensor networks, has the potential to radically improve the performance of many applications in medical, biological, and chemical fields [2], [3], [40], [41].

In our earlier work [40], [41], we have shown how a WNSN could be deployed inside a reactor for a bottom-up control of the chemical synthesis with the ultimate goal of improving the performance of the reactor. Chemical reactors are built to produce some high-value products, but they also generate some low-value materials as a by-product of some specific chemical reactions. The performance of a reactor is measured by its *selectivity*, which refers to the percentage of high-value products in the overall output [31]. By monitoring a reactor at the molecular level and turning off elementary reactions leading to undesired molecular species, a WNSN can potentially achieve very high selectivity.

An important finding of our earlier work [42] is that the packet loss in the WNSN reduces its ability to monitor and control chemical reactions, which ultimately reduces selectivity. The impact of packet loss on the selectivity depends on the chemical composition of the reactor. Interestingly, as nanomotes are expected to operate in the terahertz band [3], the absorption coefficient and the packet error rate (PER) at the receiver are also heavily influenced by the molecular composition of the reactor. However, unlike a home or an office environment, the chemical composition of the reactor varies rapidly due to the chain reactions consuming certain molecules and producing others. The time-varying composition leads to changing absorption coefficients, which in turn leads to changing PER. This means the nanomotes cannot use the same power throughout the chemical production. If the nanomotes choose to use a very high power so that they can overcome the worst possible absorption during the lifetime of the synthesis, this high power creates a high interference when the channel is good. Similarly, the nanomotes cannot choose a low power that is only suitable for good channel condition because the nanomotes will not be able to communicate when the channel is bad. For autonomous WNSNs, which are powered by limited-capacity nanobatteries [34], [35] or limited-throughput

Manuscript received May 14, 2015; revised December 18, 2015; accepted January 13, 2016. Date of publication March 2, 2016; date of current version April 5, 2016. This work was initiated while Adesoji A. Adesina was with the School of Chemical Engineering, University of New South Wales. The associate editor coordinating the review of this paper and approving it for publication was A. Eckford.

E. Zarepour, M. Hassan, and C. T. Chou are with the School of Computer Science and Engineering, University of New South Wales, Sydney, N.S.W. 2052, Australia (e-mail: ezarepour@cse.unsw.edu.au; mahbub@cse.unsw.edu.au; ctchou@cse.unsw.edu.au).

A. A. Adesina is with ATODATECH LLC, Brentwood, CA 94513 USA (e-mail: ceo@atodatech.com).

Digital Object Identifier 10.1109/TMBMC.2016.2537304

energy-harvesting circuits [36], [37], a better strategy is to adjust the power over time to maximize the selectivity with a minimal amount of power consumption. However, due to computation and communication constraints at the nanoscale, any power adaptation solution that requires the nanosensors to continuously measure the channel state would be impractical. The problem of power adaptation at nanoscale is therefore considered a very challenging task. The contributions of this paper can be summarized as follows:

- We show that the optimal power allocation for nanosensors networks trying to improve the selectivity of chemical reactors can be formulated as a Markov Decision Process (MDP) problem. The optimal power allocation enables near perfect selectivity with minimal power consumption, but difficult to realize in resource-constraint nanomotes.
- We propose offline simulation as an open-loop method to approximate the chemical process and the resulting composition over time, which enables us to derive the optimal power allocation as a function of time. The proposed method is practically realizable as the nanomotes can dynamically switch power based only on the current time without having to continuously measure the current composition.
- Using simulations of a typical gas-to-liquid process, we demonstrate that the proposed offline policy performs close to optimal achieving a three fold improvement in process efficiency with only a 100 femto watt power consumption on average. The proposed method outperforms the previously proposed open-loop power adaptation policy by 30% and the non-adaptive power allocation by 52%.

The rest of the paper is organized as follows. Related work is reviewed in Section II followed by a more detailed overview of WNSNs for chemical reactors in Section III. We present our MDP formulation and its solution in Section IV. Section V explains the proposed open-loop power adaptation policy with numerical results presented in Section VI. The feasibility of using WNSNs for chemical catalysis and realization of the proposed power allocation policy along with some future directions are discussed in Section VII. We conclude the paper in Section VIII.

II. Related Work

Much work has been done in using power allocation to combat the effect of time-varying wireless communication channel due, for example, to fading or node mobility. For example, in [24] the technique of Lyapunov optimization [29] has been extended to perform a joint optimization on routing and power allocation to provide bounded average delay in a wireless network with time-varying channel. Similarly, several attempts have been made to maximize the application layer performance via an optimum power allocation scheme in time-varying wireless sensor networks (WSNs). For instance, the papers [30] and [48] use power allocation to optimize, respectively, the mean squared error and probability of detection, in wireless sensor networks. Although these work, as well as ours, aim at using power allocation to improve the application layer performance, our performance objective is the selectivity of a chemical production process, which is a very different type of performance metric. In addition, the origin of channel variation in our work is dynamic molecular absorption in the terahertz band that is due to variation of the medium's composition within a chemical reactor.

A common technique to deal with time-varying channel is to use feedback mechanisms. There are a lot of past works in this field. We would like to highlight the work [5] which takes into account the battery power level of resource constrained device into account. However, it is not clear whether this scheme, or any other feedback-based schemes are applicable to WNSNs due to their extremely constrained energy as well as computation resources. Therefore, in this paper, we focus on deriving off-line policies that nanomotes can use without any online feedback from the channel to allow nanomotes to save their energies with only simple hardware and software.

There are a few works on power optimization for WNSNs. Jornet and Akyildiz [15] have considered the optimization of the power spectral density (PSD) of the transmitted signal over the terahertz band. In our work, we use the same molecular noise and path loss model of [15], but instead of optimizing the PSD, we consider dynamic power allocation with the aim of improving packet delivery rate which can in turn be used to achieve a better selectivity. Another distinguishing feature of our work is that, the communication channel within a chemical reactor is time-varying due to dynamic molecular absorption but the channel discussed in [15] and many other related works such as [16], [17], [18] is fixed (usually normal air). In a recent work, we have demonstrated the time-varying property of the wireless nanoscale communication within human lung as an example for in-vivo WNSN applications [47]. Taking the channel variation into the account, we then propose two duty cycling protocols to smartly put the nanomote into sleep mode when the molecular absorption in the channel is high and only wake it up and transmit when the absorption is low. Although this work uses the same concept as the current study to dynamically adapt the nanomote's behavior based on the channel's absorption but this research is different from few points of view. First, in [47] the cause of the dynamic molecular absorption in the channel is the human respiration process and the rate of variation is much lower (around few hundreds milliseconds) than the chemical reactors (around pico second). Second, in the current study, the nanomotes use a range of power levels while in [47] only one power level is used during the wake-up periods. Finally, the aim of current study is to maximize the selectivity of the chemical reactor using the minimum power budget while the main goal of the proposed protocols in [47] is to minimize the electromagnetic radiation within the human body.

Work on WNSN applications to chemical reactor performance improvement is rare with the exception of our earlier works in [40], [41], [42], where we showed how WNSN could be potentially deployed on the surface of a reactor catalyst to control and improve selectivity of the reaction process from the bottom up. In [45], we proposed frequency hopping for WNSN as a method of mitigating absorption of THz radiation in a chemically changing environment. The power allocation issue for WNSNs in the context of chemical reactors were first discussed in [43]. However, as compared with our preliminary

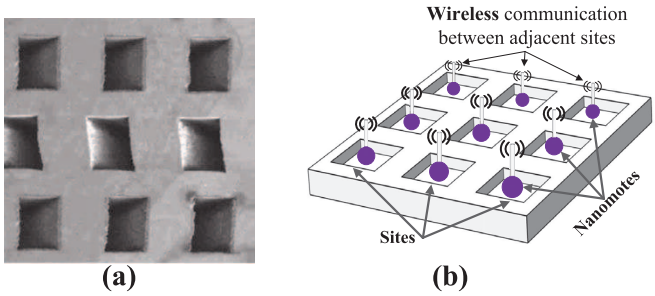

Fig. 1. (a) A scanning electron microscopy image (adapted from [26]) showing that the sites are arranged in a regular 2D grid, (b) an imaginary 3x3 nano sensor grid where each site hosts a nanomote.

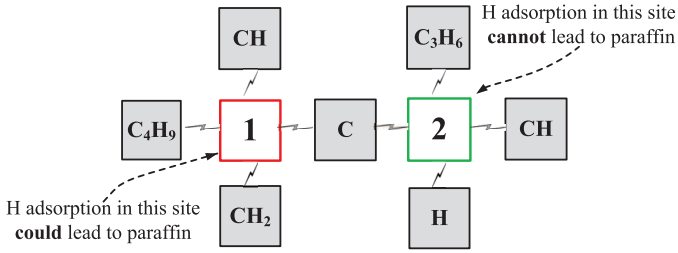

Fig. 2. Nano sensing and control on the surface of a catalyst. Nanomote in Site 1 prevents H adsorption, but the nanomote in Site 2 allows it.

conference presentation [43], this paper has considerable extensions and new materials summarized as follows. First, we have proposed and analyzed a new offline power allocation policy based on the prediction of the average expected channel composition as a function of time. We have demonstrated that the new policy significantly outperforms the best offline policy in the previous work and it is close to optimal. Second, it provides a more extensive and realistic interference model for the WNSN. Third, we provide a deeper insight to the interplay between the allocated power, the interference, and the packet error rates as a function of reactor time line, motivating the need for dynamic sensor power allocation in chemical reactors. Finally, we propose and analyze a new simple address-less protocol which requires much more simpler hardware/software to be implemented that is more beneficial for resource constraint nanomotes.

III. WNSN for Chemical Reactors

Because of their small size and unique nanomaterial properties, WNSNs can be applied in many chemical applications to monitor the chemical process at molecule level with the aim of detecting and preventing some unwanted chemical reactions. In this section, we present an overview of our earlier work [40], [41], [42] on using WNSN to improve the selectivity of chemical production. In particular, we want to highlight the connection between reliable communication among the nanomotes and the selectivity of chemical production.

Catalysts are often used in chemical reactors to speed up the reaction process. The surface of a catalyst contains numerous *sites* where reactants (molecules) adsorb and react with each other. Only one molecule can be adsorbed in an empty site at any given time and it can only react with a molecule adsorbed in another close-by site. After a reaction between two molecules in two close-by sites, a different molecule is formed in either of the two sites, making one of them empty again. This process continues until all input molecules are used up. Some composite molecules desorb from the sites, which become the (desired or unwanted) output of the reactor. Figure 1 shows a magnified view of a catalyst and a proposed WNSN with nanomotes filling up each site. Catalysts are routinely prepared in nanoscale [7], [8], [10], [21], [23], [27], [49]. This means that it may be possible to create a nanoscale manufacturing process which includes both catalyst preparation and nanomote fabrication, so that a nanomote can be embedded at each catalyst site. The manufacturing of such new type of catalyst is beyond the scope of this paper and in this paper, we assume this manufacturing process can be developed. Each nanomote is assumed to be capable of sensing the molecule type adsorbed (or attempting to adsorb) in the site, communicate with other nanomotes in the vicinity, and perform actuation to prevent adsorption of specific molecule types attempting to adsorb in the site. The mechanism required to prevent adsorption is highly dependent on the type of molecules. For example, if the molecule that we want to prevent from adsorbing has a net positive charge, then we can use a temporary positive charge to repel the molecule away from the catalyst site. This actuation mechanism is applicable to the specific chemical production process that we will discuss in the paper.

In order to give a more concrete discussion on how WNSN can be used to improve chemical production, we have chosen to use Fischer-Tropsch (FT) synthesis [1] which is a major process for converting natural gas to liquid hydrocarbons. In FT synthesis, a hydrogen atom H can react with molecules having the chemical formula C_nH_{2n+1} to form paraffins, which is an unwanted product of this synthesis. This class of reactions is known as hydrogen-to-paraffin (HTP) reactions. The aim of the proposed WNSN is to suppress the number of HTP (unwanted) reactions by ensuring that there are no hydrogen atoms near the vicinity of a C_nH_{2n+1} so that HTP reactions cannot occur. An example in Figure 2 shows that adsorption of H in Site 1 could lead to paraffin because of the presence of an C_4H_9 in the neighborhood, but its adsorption in Site 2 cannot produce paraffin. Therefore, if the nanomote at Site 1 knows that its neighboring site has a C_4H_9, it can attempt to prevent the hydrogen H atom from adsorbing into its site, preventing an HTP reaction and improving the selectivity thereby[1]. This can be realized by the nanomote at Site 1 broadcasting a query message to its neighboring nanomotes to asking them whether there is a C_nH_{2n+1} is at their sites. A neighboring nanomote should reply if it has a C_nH_{2n+1}. In order for all this to work, one important requirement is that nanomotes must be able to communicate with each other reliably. Our previous work shows that selectivity is sensitive to the packet loss in the network [42]. In the next section, we overview the relationship between communication reliability and the rate of undesired reaction in the system.

[1]What we need to prevent from adsorbing is a hydrogen ion (H^+). This can be realized by using a temporally positive charge at the catalyst site.

A. Communication Protocol

We explain earlier that our WNSN uses message exchanges between nodes to prevent undesirable reactions from taking place. In this section, we describe the required communication protocol. A nanomote broadcasts a query message to its neighboring nanomotes, which should reply if they have a molecule that can lead to an undesirable reaction. We will call the nanomote, that broadcasts the query message, the initiating node. We assume that the initiating nanomote has N neighbors. In this paper, we assume the catalyst has a regular grid structure and a nanomote can communicate with its four neighbors next to it, hence $N = 4$. Some of these neighbors have a molecule that can lead to an undesirable reaction and we will call them replying nodes because they should reply to the query message from the initiating node if they receive it. Note that the number of replying nodes is not a fixed number but depends on the chemical composition at the neighboring nodes. The message exchange is successful if the initiating node can receive at least a response from one of the replying nodes. Note that some neighbors of an initiating node may not have an "undesirable molecule at their sites; these neighbors are not replying nodes and do not need to send a reply message. Given the nanomotes have limited processing capability, we strive to create a simple protocol to realize the message exchange requirements discussed in the last paragraph. The protocol requires two types of messages: A query message from the initiating nodes and a reply message from the replying nodes. We therefore need a bit to represent these two types of messages. For node addressing, we have three options: globally unique addresses, locally unique addresses and addressless (i.e. no addresses). Since the aim of the protocol is for an initiating node to check with the nodes in its vicinity whether they have a molecule that can possibly lead to an undesirable reaction. This communication is local, so globally unique addresses with long address length can be a burden. A possibility is to use locally unique address, which is a well studied topic in traditional WSNs [14]. However, the assignment of locally unique address requires a set up phase, which adds complexity to the protocol. In this paper, we propose to use addressless messages. The messages have a length of only one bit. Specifically, the query message will consist of a single bit '0' and the reply message will consist of a single bit '1'.

We will now discuss a number of issues of the proposed single-bit protocol. The issues are: (1) A node receiving a query message does not know the identity of the sender; (2) The initiating node does not know the identity of the node sending the reply message; (3) Multiple reply nodes may send at the same time creating collision; (4) Message collision in general. The problem with Issue (1) is that a node that is not in the neighborhood of an initiating node may receive the message. This node is therefore an unintended recipient. Our intention is to use power control to limit the transmission range to minimize this from occurring. For Issue (2), we wish to point out that the initiating node does not need to know the identity of the reply nodes because the aim of the initiating node is to find out whether there is an "undesirable molecule in its neighboring sites. As long as there is an "undesirable molecule nearby, the initiating node should prevent adsorption from occurring. Given an addressless protocol, it is possible that an initiating node may receive a reply from a node that is far away, or a false positive. This false positive can lead to an initiating node to repel a molecule that is trying to adsorb. This can prevent a desirable reaction from occurring and stop an undesirable reaction from taking place. This can lengthen the time to produce the desirable products but it still achieves the goal of preventing undesirable reactions from occurring. Note that power control, which we discussed under Issue (1), can also be used to reduce the chance of false positive from occurring.

Moreover, issue (3) arises because multiple neighbors of an initiating node may have an "undesirable molecule at their sites. These multiple neighbors, or replying nodes, may reply at the same time thus causing collision. Classical methods to prevent collision include random back-off or overhearing. However, in our case, we can use physical layer modulation to make collision harmless. Specifically, at the physical layer, we assume that Pulse Amplitude Modulation (PAM) is used. We will map bit '0', which is the query message, to a pulse of lower amplitude and bit '1', which is the reply message, to a pulse of higher amplitude. If a number of reply messages reach an initiating node at the same time, the effect of the collision is to sum a number of high amplitude PAM pulses. This has the effect of making a pulse of even higher amplitude and improves the probability of correct detection. To address issue (4), we calculated the utilization of channel and found that it is generally low[2].

The above communication protocol assumes that the nanomotes use only one bit to represent a message. An alternative is to encode each message using multiple bits. This will improve the reliability of message delivery at the expense of higher power consumption. Another side effect of using multiple bits is that it increases the round-trip delay for the communication between a querying node and a replying node, which may subsequently affect the control performance.

B. Effect of Communication Reliability

In this section, we model the reliability of the message exchange protocol and its effect on the application performance. Let f be the probability a neighboring node is a replying node. The probability that there are i replying nodes in the neighborhood is $P(N, i) = \binom{N}{i} f^i (1-f)^{N-i}$ and the probability that there is at least one replying node is $\sum_{i=1}^{N} P(N, i)$. A message exchange between the initiating node and replying nodes is successful if the initiating node receives a reply from at least one of the replying nodes. Let p denote the packet error rate (PER), which is assumed to be the same in both directions

[2]For example, for FT synthesis with initially 10^5 CO molecules, 2.5×10^5 atoms and 10^4 sites, the probability that a node will initiate a query is $p_{\text{query}} = 0.42$ and the probability that a neighboring node will reply is $p_{\text{reply}} = 0.37$. The average reaction rate (counting all reactions) at a site is $r = 10^8$ reactions/s, therefore query messages are generated at a rate of $p_{\text{query}} r$ messages/s and reply messages are generated at a rate of $n_{\text{neighbor}} p_{\text{reply}} p_{\text{query}}$ messages/s where $n_{neighbor} = 8$ is the number of neighboring nodes. Each message has a length of 1 bit and the bit duration is $t_{\text{bit}} = 10^{-13}$ seconds [18]. The utilization of the channel is $(1 + n_{\text{neighbor}} \times p_{\text{reply}}) \times p_{\text{query}} \times r \times t_{\text{bit}} = 10^{-5}$.

of message exchange. This means that the message exchange between an initiating node and a replying node fails with a probability $q = 1 - (1 - p)^2$. If an initiating node has i replying nodes in its neighborhood, then the probability of a successful message exchange between an initiating node and at least one of i replying nodes is $(1 - q^i)$. Finally, the probability s of successful message exchange given that there is at least one replying node is:

$$s = \frac{\sum_{i=1}^{N} P(N, i)(1 - q^i)}{\sum_{i=1}^{N} P(N, i)} \tag{1}$$

The application layer performance of our WNSN depends on how much the undesirable reactions can be suppressed. Let k denote the reaction rate of an undesirable reaction in the chemical reactor. It can be shown that the rate of undesirable reactions is reduced to $k(1 - s)$ where s is the conditional probability of successful packet exchange in Equation (1). In particular, if the probability of successful message exchange s is high, then the undesirable reaction rates are much reduced. This derivation shows the connection between message exchange reliability and application layer performance of the WNSN.

The expression for successful message exchange probability s depends on three parameters N, f and p. The number of neighbors N is the number of neighboring nodes that an initiating node needs to broadcast query message to. This is defined by the application requirement and we assume $N = 4$ in this paper. The probability f that a node is a replying node depends on what type of molecules a node has. This probability is not fixed but varies with time. Recalling that a replying node must contain a particular precursor of undesirable chemical reactions, we will use the ratio these precursors at any given time as the probability f at that time. The packet loss probability p depends on the radio channel, which in turns depends on the transmission medium. As nanotransceivers operate in the terahertz band, the packet lost probability is strongly affected by molecular absorption noise and attenuation in the terahertz channel [15]. On the other hand, due to extremely dense structure of the proposed WNSN in the surface of the catalyst (trillions of sites), the interference due to concurrent radiation of other nodes may affect the quality of the communication. In the next section, we will review the WNSN's channel over terahertz band and also model the interference in the system.

C. WNSNs Radio Channel

As nanoantennas are operating in the terahertz band ranging from 0.1-10 THz [19], the wireless medium between the nanoantennas is mainly affected by the produced molecules during the chemical reactor, both adsorbed/formed molecules in the sites and desorbed species. This section therefore reviews the modeling of terahertz radio channel based on radiative transfer theory presented in [15]. We assume the radio channel is a medium consisting of N chemical species $S_1, S_2, \ldots, S_N$. The effect of each chemical species S_i on the radio signal is characterized by its molecular absorption coefficient $K_i(f)$ of species S_i at frequency f. The molecular absorption coefficients of many chemical species are available from the *HITRAN* database [4]. We consider a radio channel in a chemical reactor which has time-varying chemical composition. Let $m_i(t)$ be the mole fraction of chemical species S_i in the medium at time t. The medium absorption coefficient $K(t, f)$ at time t and frequency f is a weighted sum of the molecular absorption coefficients in the medium:

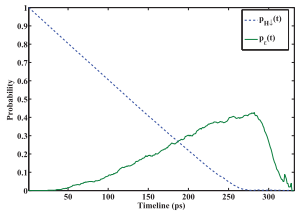

(a) Average medium absorption coefficient over terahertz band.

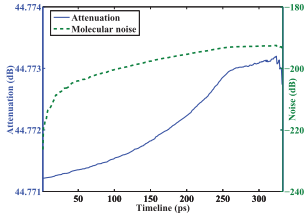

(b) Molecular absorption noise and total attenuation.

Fig. 3. Medium status during FT synthesis.

$$K(t, f) = \sum_{i=1}^{N} m_i(t) K_i(f) \tag{2}$$

We obtain the chemical composition $m_i(t)$ of the FT chemical reactor by using the stochastic simulation algorithm (SSA) [12], which is a standard algorithm to simulate the chemical reactions. We assume an initial composition of 100 Carbon Monoxide molecules (CO) and 250 Hydrogen atoms (H) and use 100 runs of SSA simulations. Figure 3a shows the average absorption coefficient of the radio channel, over terahertz band ranging from 0.1 to 10 THz, within a FT reactor. It shows that the absorption coefficient of the medium increases exponentially which is due to the presence of some extremely high absorbent intermediate species, such as OH, in the medium. $K(t, f)$ determines the attenuation and the molecular absorption noise in the radio channel. The total attenuation $A(t, f, d)$ due to spreading and molecular absorption at time t, frequency f and a distance d from the radio source would be [15]:

$$A(t, f, d) = \left(\frac{4\pi f d}{c}\right)^2 e^{K(t,f)d} \tag{3}$$

A discussion on time-scale is warranted here because the medium absorption coefficients $K(t, f)$ has a transient time and $K(t, f)$ also depends on the chemical composition, which varies over time. In [22], the medium absorption coefficients $K(t, f)$ is shown to have a transient time of around 0.05 ps. In [46], the mean time between two chemical reactions is shown to be in the order of picoseconds. This means that we can ignore the transient time of $K(t, f)$ and assume that $K(t, f)$ follows the changes in composition of the propagation medium.

Let $U(t, f)$ be the power spectral density of the transmitted radio signal at time t and frequency f. The received signal at time t, frequency f and distance d is:

$$P_r(t, f, d) = \frac{U(t, f)}{A(t, f, d)} \tag{4}$$

The average received energy for a given reaction of r_i at time t then would be:

$$E_r(t, d) = \int_B P_r(t, f, d) T_p df \tag{5}$$

where T_p is the duration of the transmitted pulse in second (here $T_P = 10^{-13}$).

The molecular absorption noise $N_{\text{abs}}(t, f, d)$ which is due to the re-radiation of absorbed radiation by the molecules in the channel is given by [15]:

$$N_{\text{abs}}(t, f, d) = k_B T_0 (1 - \exp(-K(t, f) * d)) \tag{6}$$

where T_0 is the reference temperature 296K and k_B is the Boltzmann constant. Figure 3b shows the attenuation and PSD of the molecular absorption noise during an FT synthesis.

Finally, for simplicity, we have not taken into consideration the effects of reflection and diffraction in the radio model, because precise study of these effects will require the geometry of the catalyst and that of the chemical reactor. Given that the focus of this paper is on developing methodologies for open-loop power adaptation, we remark that the proposed methodologies are independent of the radio model. In other words, the methodologies are also applicable when a radio model that takes into account reflection and diffraction is used.

D. Receiver Model

We assume the distance between two direct neighboring nodes is d_0. As we have discussed in section III.A, we use PAM to modulate the exchanged messages, so the receiver consists of a simple energy detector (ED) with two thresholds to detect the noise, query and reply. At any time slot t, we assume each nanomote uses $P_{T,0}(t)$ and $P_{T,1}(t)$, respectively to transmit a query and reply, where $P_{T,0}(t) < \alpha P_{T,1}(t)$ and $\alpha < 1$ is a design parameter and we have chosen $\alpha = 0.5$. Note that this choice of α decreases the probability of a receiver mistaking a query message as a reply message. We assume that all nanomotes use the power levels $P_{T,0}(t)$ and $P_{T,1}(t)$ at time t; the determination of these power levels are discussed in Section V.

The ED requires the design of a filter, matched to the received pulse shapes. We assume the bandwidth of the filter is equal to $B = 10^{13}$. If a nanomote transmits a pulse with the total transmitted power of $P_{T,i}$ then the received energy level at the receiver has a Gaussian distribution of $g_i(t)$ with mean $\mu_i(t)$ and variance $\sigma_i^2(t)$ given by [6]:

$$\mu_i(t) = N(t) \times T_{\text{int}} \times B + E_{r,i} \tag{7}$$

$$\sigma_i^2(t) = N^2(t) \times T_{\text{int}} \times B + 2N(t) \times E_{r,i} \tag{8}$$

where N is the noise PSD at distance d_0 that can be calculated from equation 6, $E_{r,i}$ is the average received energy for pulse i at distance d_0 that can be calculated from equation 5 and T_{int} is the integration time which is a design parameter, typically $T_{int} >= T_p$.

The first threshold that is used to detect queries from the replies at time t, $\xi_{0,1}(t)$, is given by the intersection of the Gaussian density functions with parameters $(\mu_0(t), \sigma_0^2(t))$ and $(\mu_1(t), \sigma_1^2(t))$. In order to distinguish noise from a query, we define a second threshold of $\xi_{n,0}(t)$ which $\xi_{n,0}(t) = \beta \xi_{0,1}(t)$, where $\beta < 1$ is a design parameter.

E. Interference Model

Now, we turn to investigate the interference in the channel which is due to concurrent transmission from other nodes. The interference at time t and frequency f, can be calculated as:

$$I(t, f) = \sum_{x=1}^{M} Tr_x(t) P_R(t, f, d_x) \tag{9}$$

where M is number of interfering nodes which depends on the topology structure of the WNSN[3], $P_R(t, f, d_x)$ is the received power from the interfering node x at frequency f and time t that can be calculated via Equation (4). The interfering node x is in a distance equal to d_x and transmits with a probability Tr_x. In [43], we assumed a fixed transmission probability for all nodes during the synthesis. However, transmission probability $Tr(t)$ at a given time t depends on the probability of an initiating node broadcasting a query, $p_q(t)$, and the probability of replying nodes sending a responses, $p_r(t)$, which are both time dependent. Here, we propose a more realistic model for transmission probability.

Without loss of generality, we assume that the undesirable reactions, that the WNSN aims to prevent, involve an H atom and an E molecule. When an H atom tries to adsorb at an empty site, the nanomote at the site becomes an initiating node and broadcast a query message to its neighboring nanomotes. If any one of the neighboring nanomotes has an E molecule, they become the replying nodes and send the initiating node a response. In order to compute the message exchange probability, we need to determine $p_{H\downarrow}(t)$ and $p_\epsilon(t)$, which are, respectively, the probabilities that an H atom tries to adsorb at an empty site and there is an E molecule in the neighborhood. The probability $p_{H\downarrow}(t)$ can be obtained from the number of unadsorbed H atoms in the reactor at time t using simulation. The probability $p_\epsilon(t)$ is:

$$p_\epsilon(t) = \sum_{i=1}^{M} \binom{M}{i} f(t)^i (1 - f(t))^{M-i} \tag{10}$$

where $f(t)$ is the probability that any of the M neighbors has an E molecule at time t. The probability $f(t)$ can be determined from the ratio of E molecules in the chemical reactor at time t using simulation. Note that $f(t)$ in this section has the same meaning as the $f(t)$ in Section III-B. We can compute the transmission probability $T_r(t)$ of an interfering node as:

$$T_r(t) = p_q(t) + p_r(t) \tag{11}$$

$$= p_{H\downarrow}(t) + p_{(\epsilon \text{ and } H\downarrow)}(t) \tag{12}$$

$$= p_{H\downarrow}(t) + p_\epsilon(t) \times p_{H\downarrow}(t) \tag{13}$$

[3]In order to determine M, we make the following assumptions: (1) The sites form a regular grid on the catalyst surface; (2) A nanomote intends to communicate with the 4 neighbors next to it and the communication range (= one hop) is the distance between 2 nodes on the grid; (3) The interferers are all the nodes 2 hops away. Based on these assumptions, the number of interferer is $M = 16$.

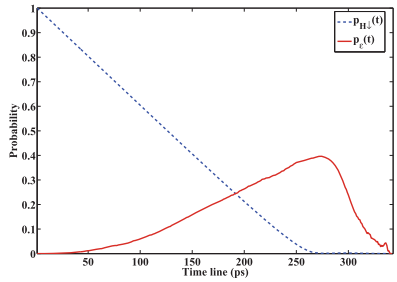

(a) Probability that a hydrogen atom is trying to adsorb into an empty site and the probability of existing an E molecule (C_nH_{2n+1}) during a FT synthesis.

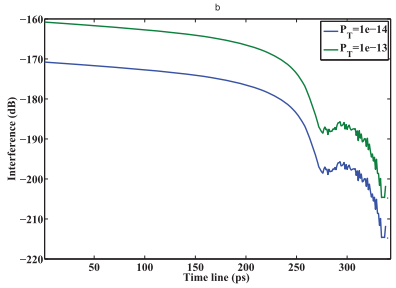

(b) The interference due to transmission of other nodes for two transmission powers.

Fig. 4. Transmission probability and interference during FT synthesis (M=16).

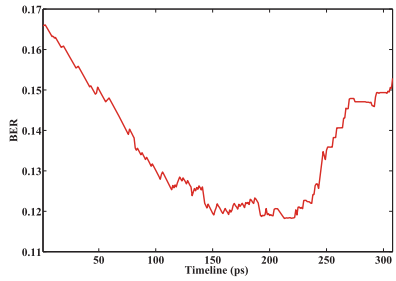

(a) BER during one run for a transmission powers equal to 30fW.

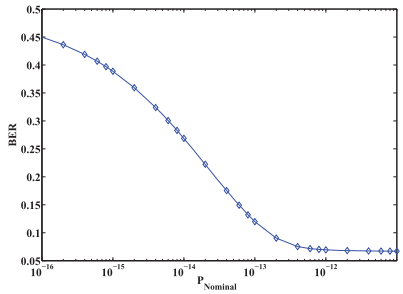

(b) Average BER during the whole process over 10 simulation runs for 30 different transmission powers

Fig. 5. Packet error rate within FT reactor.

Figure 4b shows $p_{H\downarrow}(t)$ and $p_\epsilon(t)$ during the FT synthesis. For the initialization of the simulation, we assume the number of unoccupied sites at the beginning of the reactor is equal to the initial number of hydrogen atoms. As it can be seen, $p_{H\downarrow}(t)$ dramatically drops due to consumption of the hydrogen and also decreasing number of unoccupied sites due to forming other species. On the other hand, $p_\epsilon(t)$ increases because of the formation C_nH_{2n+1} (which we simply call E earlier). Using Equations (9) and (13), we can calculate the resulting interference during the FT synthesis and the results are depicted in Figure 4b. It shows the interference is decreasing over time due to increasing molecular attenuation over time (see Figure 3b).

F. Reliability Analysis

The signal to interference-noise ratio (SNIR) at time t, frequency f and distance d is:

$$\text{SNIR}(t,\, f, d) = \frac{P_R(t,\, f, d)}{(N_{\text{abs}}(t,\, f, d) + I\,(t,\, f))} \tag{14}$$

Assuming nanomotes are using binary PAM for message exchange, we calculate the Bit Error Rate (BER) from SNIR. Note that as the packet length is equal to one, BER and PER have the same meaning. Figure 5a shows the BER during one course of FT synthesis for a transmission power equal to $3 \times 10^{-14} W$. It shows that BER starts at around 0.165 and then fluctuated during the synthesis due to variation in the molecular noise and interference over time. It also highlights the need for dynamic power allocation to provide reliable communication in the channel. Figure 5b presents the average BER during the FT synthesis for 30 transmission powers ranging from 10^{-17} W to 10^{-11} W which each point represents the average BER over 10 runs simulation for the previous setting. It shows that by increasing the transmission power from 0.01fW to 0.5pW the BER drops from 0.7 to around less than 0.05 but further increasing does not decline the BER due to high interference. In the next section, we develop an analytical model to dynamically adjust the transmission power with the ultimate goal of increasing selectivity with the minimum power allocation.

IV. MDP for Dynamic Power Allocation

In Section III, we describe how a WNSN can be used to improve the selectivity of a chemical production by suppressing those undesirable chemical reactions that lead to low value products. We also explain that the efficacy of suppressing the undesirable reactions depends on the PER between neighboring nodes in the WNSN. The PER depends on the transmission power, path loss, molecular absorption noise and interference. The latter three factors depend on the chemical composition of the transmission medium [15], which is constantly changing in a chemical reactor because of production and consumption of chemical molecules. Therefore, if the nanomotes use a constant transmission power, the PER will change over time and this can affect the selectivity. An alternative strategy is for the motes to adjust their transmission power to keep the PER low. However, given the limited energy budget of an autonomous WNSN, the transmission power has to be appropriately adjusted to give maximum improvement in selectivity. In this section, we show that this dynamic power allocation problem can be formulated

as an MDP. In section IV-A, we use a simple example to illustrate how an *uncontrolled* chemical reaction can be modeled by an embedded Markov chain (EMC). The aim of this section is to draw a connection between state transition probability and reaction rates. Given that the goal of our WNSN is to control the reaction rates, which is related to the state transition probability, therefore the power allocation problem can be formulated as an MDP. In section IV-B, this MDP will be defined.

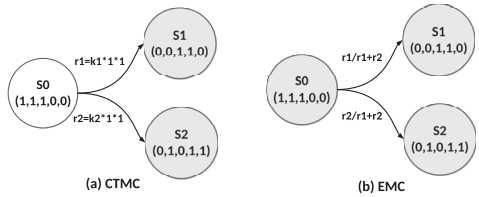

Fig. 6. CTMC and EMC of a simple set of chemical reactions.

A. Markov Chain for Uncontrolled Chemical Reactions

The paper [13] proves that the dynamics of a set of chemical reactions can be modeled by a continuous-time Markov chain (CTMC). We use a simple example to illustrate the idea. In particular, we want to show how the states and transition probabilities are defined. This will help us to define the MDP problem in the next section. We consider a chemical reactor with 3 input chemical species A, B and C. Two possible chemical reactions can take place in this reactor. In the first reaction, a molecule of A reacts with a molecule of B to form a molecule of D; this is commonly expressed using the chemical formula of $\mathrm{A} + \mathrm{B} \rightarrow \mathrm{D}$. The second reaction is $\mathrm{A} + \mathrm{C} \rightarrow \mathrm{E}$. We use n_X to denote the number of molecules of chemical species X. The state of the chemical reactor is the 5-tuple $(n_A, n_B, n_C, n_D, n_E)$. That is, the state consists of the number of each type of molecules in the chemical reactor. For simplicity, we assume the initial state of the reactor is $S_0 = (1, 1, 1, 0, 0)$ which means there is a molecule of A, B and C and no molecules of D and E. If the reaction $\mathrm{A} + \mathrm{B} \rightarrow \mathrm{D}$ occurs, then the state will transit from S_0 to $S_1 = (0, 0, 1, 1, 0)$ with one molecule of C and D. Similarly, if $\mathrm{A} + \mathrm{C} \rightarrow \mathrm{E}$ occurs, then the state will become $S_2 = (0, 1, 0, 0, 1)$. Given the initial state S_0, it can be seen that S_0, S_1 and S_2 are all the allowable states. These are the states of the CTMC, see figure 6(a). The transition rate of the CTMC is governed by the rate of chemical reactions. For reaction $\mathrm{A} + \mathrm{B} \rightarrow \mathrm{D}$, the reaction rate is $r_1 = k_1 n_A n_B$ where k_1 is the kinetic constant of this reaction and a larger k_1 means a higher likelihood for the reaction to occur (= high state transition rate). Note also that the reaction rate depends on the state. The transition rate from S_0 to S_1 is r_1. Similarly, the transition rate from S_0 to S_2 is $r_2 = k_2 n_A n_C$. The CTMC is now completely defined and is illustrated in figure 6(a). In order to leverage the theory of MDP to solve the power allocation problem, we convert the CTMC to an Embedded Markov Chain (EMC) [32]. Figure 6(b) illustrates the EMC of the CTMC in figure 6(a). The states of the EMC are the same as those of CTMC. However, the transition rates have been replaced by transition probability. In particular, for our example, the transition probabilities from S_0 to, respectively, S_1 and S_2, are, $\frac{r_1}{r_1+r_2}$ and $\frac{r_2}{r_1+r_2}$. In general, if the transition rate from state S_i to S_j in a CTMC is q_{ij}, then the transition probability from state S_i to S_j in the corresponding EMC is $\frac{q_{ij}}{\sum_j q_{ij}}$ if $i \neq j$ and is zero otherwise.

B. MDP Formulation

We now present an MDP formulation for the dynamic power allocation problem for the FT reactions.

1) States: The state of the FT process consists of the number of each type of molecules in the FT process. For illustration, Figure 9b shows the EMC for the *uncontrolled* FT process where the initial state S_0 consists of 2 carbon (C) and 4 hydrogen (H) atoms. The process consists of altogether 9 different states with different chemical compositions in each state. The transition probability of the EMC has been calculated from the corresponding CTMC using the method described earlier.

The states S_6 and S_8 of the EMC are the absorbing states. When the FT process reaches any one of its absorbing states, we assume the chemical production is complete. The chemical composition of the absorbing state is important. If an absorbing state consists of a larger quantity of high value product, then the selectivity of that state is high.

2) Actions: We assume that at each state, m different transmission power levels $P_1, P_2, \ldots, P_m$ are available for the nanomotes to use. The actions of the MDP are these different power levels. This can be viewed as a cross-layer optimization where physical layer parameter (in our case, power) is used to maximize selectivity, which is an application layer performance.

We will use the EMC in figure 7 to explain the effect of the actions. Our discussion focuses on state S_4. This state can transit to states S_2, S_6 and S_7. The probability of transiting to each of these states in the (uncontrolled) EMC is the same (=0.33). This also means that the transition rates from S_4 to any one of these states in the corresponding CTMC is the same and we will denote it by r. Out of these three transitions, the move from S_4 to S_6 produces a molecule of CH_4, which is a low value paraffin. The aim of the WNSN is to suppress this reaction as much as possible. Let us assume that the probability of successfully suppressing this reaction by the WNSN is p, then WNSN reduces the transition rate from S_4 to S_6 from r to $(1-p)r$. The reaction rates from S_4 to states S_2 and S_7 will not be altered by the WNSN because no undesirable products are produced. With the revised reaction rate due to the actions of WNSN, the transition probability from S_4 to S_6 reduces from 0.33 to $\frac{1-p}{3-p}$ in the (controlled) EMC. This shows how the *probability of successful suppression* affects the state transition probability.

The probability of successful suppression p depends on many factors, including those related to efficiency of sensors and actuators. In this paper, we assume that p is the same as the probability that sensors from neighboring sites are able to successfully communicate with each other. Hence p is a function of the transmission power, which are the actions of the MDP. At the same time p depends on molecular absorption, which is a function of the chemical composition. Recalling that each state of the MDP is defined by the chemical composition, therefore p

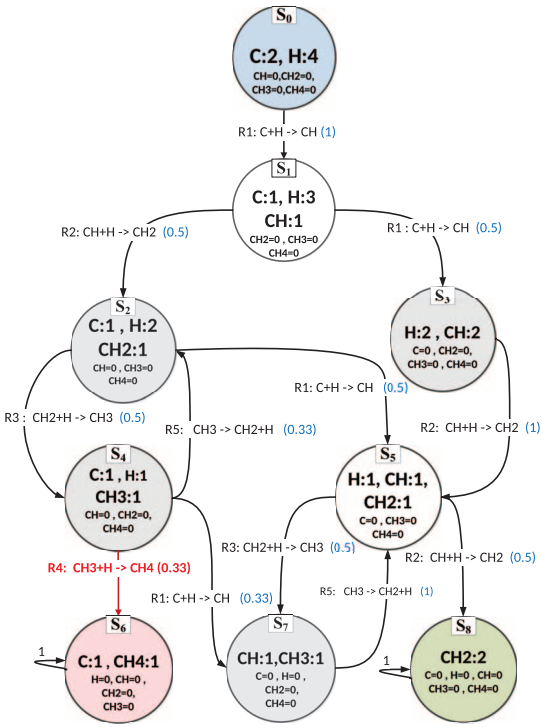

Fig. 7. EMC for the FT process with an initial state of 2 carbon and 4 hydrogen atoms. S6 and S8 are absorbing states. The blue number in the parentheses are probability of transition from one state to another state. WNSN aims to reduce the rate of HTP reactions, e.g., in this example the WNSN tries to reduce probability of going from state 4 to state 6.

is state dependent. Finally, p is also affected by interference due to other nanomotes' transmissions. This interference depends on nanomotes' transmission power and also the composition. To sum up, a chosen transmission power at a given state will give rise to a certain PER, which can in turn affect selectivity.

For the MDP for dynamic power allocation, the actions are the m different power levels. For each power level, we can compute the resulting state transition probability in the EMC similar to that described earlier. Note that the calculation takes into account the transmission power and channel condition, which is state dependent.

3) Revenue Function: The revenue is a function of two quantities, the power level (P_i) chosen and r_i, the total rate of HTP reactions resulting by selecting P_i, where $r_i => 0$ and P_i is within the range 10^{-18} to 10^{-12}. Increasing r_i and P_i should have a negative effect on revenue (or selectivity), and vice versa. This can be captured via different types of functions. Because P_i has a wide range, we define the function as:

$$Revenue_i = \underbrace{(1 - r_i)}_{\text{Reward}} + \underbrace{\frac{k}{\log(P_i)}}_{\text{Penalty}}$$

where k is a design parameter to control the penalty. Here we use $k = 0.1$. Note: because $P_i < 1$ then $\log(P_i)$ is always negative.

C. Large Scale MDP

The number of states in the FT process increases exponentially with the number of initial atoms. For example, for the initial gas feed comprising only 10 carbon and 20 hydrogen atoms, we obtain in excess of 35,000 states. For a feed gas with large number of carbon and hydrogen atoms, we face a state explosion problem, which makes it difficult to solve the MDP problem and obtain the optimum policy within a reasonable time.

There are several attempts in the literature to alleviate the MDP state explosion by techniques such as state space reduction and other approximation methods. Kearns et al. [20] proposed a *sparse sampling algorithm* which yields a near-optimal outcome for a large or infinite MDP. In order to implement this algorithm in our context, we start with an initial state with a given number of carbon and hydrogen atoms and then as long as an absorbing state has not been reached, the following steps are executed for each state S_i reached:

1) Calculate the revenue for all possible actions (power levels)
2) Select the action with maximum revenue and call it P_{opt_i}.
3) Use the state transition probabilities for action P_{opt_i} to randomly follow one of these state transitions and move to the next state based on the selected transition. Go back to 1 if the new state is not absorbing.

Note, that the algorithm does not attempt to solve the MDP problem, i.e., it does not attempt to find an (optimum) action for every possible state. Instead, it produces a trace of states and associated power levels from the initial state to the absorbing state, which is then used to derive selectivity and average power level.

V. Local Power Allocation Policies

MDP provides the optimal power allocation policy, but requires the nanomotes to know the *global* state, or the exact chemical composition, of the chemical reactor. This is not a practical policy because it requires each nanomotes to broadcast its local state in the WNSN, which would consume a lot of energy. In this section, we investigate the possibility of each nanomote executing the same local pre-planned (or open loop) policy where the transmission power is adjusted over time. A pre-planned policy of X can be expressed as a univariate function $t \mapsto P_X(t)$ where $P_X(t)$ specifies the power level that the nanomotes should use at time t. In this section, we describe two local polices. Section V-A describe a local policy derived from HTP reaction rate and receiver noise; this policy is the best performing local policy proposed in [43]. Section V-B presents a new local policy based on average composition. We will compare the performance of these two policies against the optimal MDP policy in Section VI.

A. A Local Policy Based on Reaction Rate and Noise

Since the goal of the WNSN is to reduce the number of HTP reactions (the undesirable reactions) in the FT reactor, a possible policy is for the nanomotes to reserve the transmission power when the HTP reactions are more likely to

occur so as to increase the chance of suppressing them. At the same time, a nanomote needs to exchange messages with its neighbors to know whether an HTP reaction may occur. Given that communication is a requisite, a possible policy is to allocate power according to the amount of noise in the transmission medium. In [43], we study the performance of three local policies. One local policy allocates more power to the nanomotes when the rate of HTP reaction is high. The second local policy allocates more power to the nanomotes when the noise in the transmission medium is high. Neither of these policies performed very well because they consider only one aspect of the problem. The best policy in [43] allocates power using both the HTP reaction rate and noise in transmission medium. This local policy is to use high transmission power when *either* reaction rate *or* noise is high. We will refer to this policy to as reaction-rate and noise local policy (RR+NLP). The details of deriving this policy from the HTP reactions rate and transmission medium noise can be found in [43].

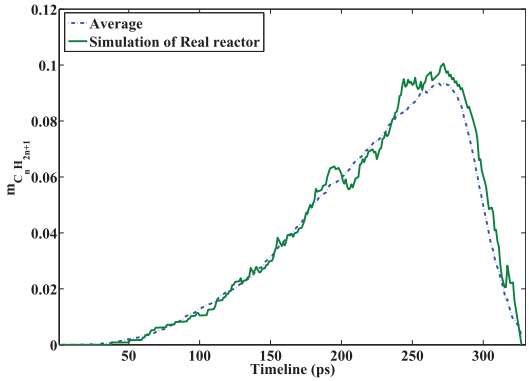

Fig. 8. Evolution of the mole fraction of C_nH_{2n+1} from both $\vec{s}_{\mathrm{AVG}}(t)$ via 100 SSA runs and also a single simulation of the FT reactor.

B. A New Local Policy Based on Average Composition

In this section, we propose a local policy based on average composition of the reactor over time. The policy is based on solving an MDP based on the average composition of the reactor over time and we refer to this offline policy as ACLP (Average Composition Local Policy). For the time being, we will assume that the average composition is available and will describe later on how it can be computed.

We assume the chemical reactor has Q chemical species $S_1, S_2, \ldots, S_Q$. The quantities of these chemical change over time as they are consumed or produced. The chemical composition of the reactor at time t is defined as the number of molecules of each chemical species at the time. We will use a vector $\vec{s}$ to store the chemical composition because there are multiple chemical species in the reactor. Let $\vec{s}_{\mathrm{AVG}}(t)$ $(t = 1, 2, 3, \ldots)$ denote the average composition of the reactor at time t. We define a Markov chain with these two attributes: (1) The state space is $\mathcal{S}_{\mathrm{AVG}} = \{\vec{s}_{\mathrm{AVG}}(1), \vec{s}_{\mathrm{AVG}}(2), \vec{s}_{\mathrm{AVG}}(3), \ldots\}$; (2) The transition probability from $\vec{s}_{\mathrm{AVG}}(t)$ to $\vec{s}_{\mathrm{AVG}}(t+1)$ is 1 while all other transition probabilities are zero. We now define a MDP over this Markov chain using the same MDP action set and objective function as in Section IV-B. The solution of this MDP gives us the power level $P(t)$ to be used at time t. The ACLP is to use the power level $P(t)$ at time t.

The calculation of $\vec{s}_{\mathrm{AVG}}(t)$ can in principle be performed analytically by solving a Chemical Master Equation (CME) of the reactor. However, this is practically impossible because the size of the state space $\mathcal{S}$ is exponential in terms of the number of molecules in a reactor, which is generally large. We therefore choose to use SSA simulation to obtain the average composition at time t as $\vec{s}_{\mathrm{AVG}}(t) = \frac{\sum_{i=1}^{J} \vec{s}_i(t)}{J}$, where J is the number of times SSA is run, and $\vec{s}_i(t)$ is the composition in time slot t for the i-th simulation run[4].

[4]As different simulation runs have slightly different lengths, we choose to truncate all simulation outputs to the minimum of all simulation runs.

We will show in Section VI that this local policy performs close to the optimal MDP that uses the actual state (= chemical composition) of the reactor. The reason why this policy performs well is that the actual chemical composition of the reactor can be well approximated by the average chemical composition, which we confirm using 100 runs of SSA. Figure 8 plots the average/single realization of a given chemical specie (C_nH_{2n+1}) over time and provides a visual confirmation that average is a good predictor for reactor composition. In fact, over 330 time slots, the average difference between these two composition-time curves is only around 12%.

The main challenge with the proposed simulation-based derivation of $\vec{s}_{\mathrm{AVG}}(t)$ is the complexity of the simulation, which is directly dependent on the number of states, that in turn depends on the volume of input gas. One way to address the scalability issue with simulation complexity would be to simulate a small-scale process and use the derived optimal power allocations for each single time slot to approximate power allocation of a group of X slots in the large process, where X is the ratio of the length of the large process to that of the small process. As we will demonstrate in Section VI, this approximation can retain the selectivity and power consumption within 5% of the small-scale process even with a 1000x increase in process length ($X = 1000$). Note that there are efficient computation algorithms to perform SSA simulations. For example, the Next Reaction Method [11] has a complexity of $O(n_{\mathrm{edges}} + \log(n_{\mathrm{reactions}}))$ where $n_{\mathrm{reactions}}$ is the number of reactions, and n_{edges} is the number of edges of a dependency graph and typically n_{edges} is much smaller than $n_{\mathrm{reactions}}$.

We will end this section by discussing how the local policy may be implemented. The computation of the local policy will be performed offline. Once the local policy has been determined, it will be loaded into the memory of the nanomotes in the form of a lookup table. The lookup table has two "columns: time and the power level to be used at that time. We assume that each nanomote has its own clock and looks up the power needed for each time. This means that the nanomotes do not need to do any calculations and are only required to perform lookup operations.

VI. Results

This section aims to study the performance of the local policies proposed in section V. A good policy is one which produces a higher selectivity for a given power budget. We compare these local policies against the MDP policy and constant power allocation. Note that the MDP policy is the optimal policy but it is not feasible to implement in nanomotes because it requires the exact composition of the reactor at each time instance.

A. Simulation Set Up and Methodology

We assume the FT synthesis starts with 100 carbon monoxide molecules and 250 hydrogen atoms. The chemical production continues until no more new chemicals can be produced. The reactor is assumed to operate at a temperature of 500K and pressure of 10 atmospheres. The nanomotes operate in the terahertz band ranging from 0.1–10 THz and use binary PAM as their modulation schema. The pulse duration is 100fs and the probabilities of bit 1 and bit 0 are assumed to be equal. The molecular absorption noise in the reactor depends on the chemical composition within the reactor. We follow the procedure of section III-C to compute the molecular absorption noise/attenuation, signal to noise-interference ratio and finally PER.

The distance between two neighboring nanomotes is assumed to be 1 μm. Although the quality of terahertz nanoscale communication in normal air up to few millimeter might be promising [18], communication within a FT reactor even in 1 μm is challenging. This is because during the course of FT synthesis, some intermediate species (e.g., hydroxide, OH) which have very high absorption coefficients, are produced. In fact, the average absorption coefficients of these chemical species over the terahertz band are a few order of magnitudes greater than the average absorption coefficient of the channel with normal air composition which finally increase the absorption coefficient of the FT medium, dramatically. For example, as it can be seen from Figure 3a, the maximum average absorption coefficient of the FT medium in the working pressure/temperature of the reactor (10atm/500K) is more than $650m^{-1}$ while the average absorption of the normal air in the normal pressure/temperature (1atm/300K) is only $6\,m^{-1}$; this is a more than 100-fold difference. We conduct 20 sets of experiments, each with a different nominal power levels P_{nominal} chosen from 10^{-16} to 10^{-12} W. The schemes to be compared are constant power allocation, MDP, RR+NLP (which is the best local policy proposed in [43]) and ACLP (our new local policy). We now explain how these schemes make use the nominal power level. For constant power allocation, each nanomote uses P_{nominal} as the transmission power. For other policies, we generate m discrete power levels. The minimum power P_1 is zero which means the nanomotes do not communicate. The other $m-1$ power levels are drawn from $[\frac{P_{\text{nominal}}}{1000}, P_{\text{nominal}}]$ with maximum power $P_m = P_{\text{nominal}}$ and that have been equally spaced in this range. These m power levels are used by the MDP and the local polices. Here, we use $m = 30$. For a selected transmission power level P_T, the nanomotes use $\frac{1}{2}P_T$ and P_T to transmit, respectively, a query ($P_{T,0}$ in Section III-C) and a reply ($P_{T,1}$). At any given time slot t, we follow Section III-C to calculate the receiver's thresholds $\xi_{0,1}(t)$ and $\xi_{n,0}(t)$.

For MDP, we use the sparse sampling method to compute selectivity and average power usage. For constant power allocation and local policies, we incorporate the power selection into the transition rates of the CTMC describing the FT process. We can therefore simulate these by using SSA. At the end of each simulation, we compute the selectivity and the *average* power usage for that simulation run. Note that the *average* power usage for MDP and the local policies can be *different* from the nominal power. For each of these policies, we repeat the simulations five times and then average the results over the five simulation runs to obtain the final results.

B. Results and Discussion

First, we present the power allocation policy computed by MDP and show its ability to reduce the number of HTP reactions. The results are obtained for a nominal power of 49fW. As a reference, we plotted the probability of HTP reactions $\rho_U(t)$ at time t in an uncontrolled reactor in Figure 9a. The graph shows that for uncontrolled reactor, the maximum HTP reaction probability is 0.28. Figure 9b shows the MDP power allocation policy $P_{\text{MDP}}(t)$ as well as the probability of HTP reaction $\rho_{MDP}(t)$ when the MDP policy is used. Note that $\rho_U(t)$ in Figure 9a and $\rho_{MDP}(t)$ in Figure 9b are plotted using the same scale. It can be seen that the probability of HTP reactions is significantly reduced by the MDP policy. In particular, the MDP policy reduces the maximum probability of HTP reactions to 0.07. The MDP policy leads to a selectivity of 0.87 with average consumed power of 49×10^{-15}. Figure 9c shows the receiver thresholds $\xi_{0,1}(t)$ and $\xi_{n,0}(t)$ for $\beta = 0.2$. The application layer performance of our WNSN is measured by the selectivity. We study the achieved selectivity for 4 different policies (MDP, RR+NLP, ACLP and constant) by varying the nominal power. Figure 10 shows the selectivity versus average power for the four policies and we have also added the selectivity of the uncontrolled reactor as a reference. It shows that all four policies can improve the selectivity. Among them, MDP policy is always the best and constant is always the worst. For the two local policies, ACLP is always better than RR+NLP. Moreover, for a certain range of nominal power, ACLP achieves a selectivity close to that of MDP. We also find that irrespective of the policy, the selectivity is optimized for an average power allocation of around 100fW[5]. ACLP achieves a maximum selectivity of 0.91, which is within 1% of that obtained by MDP. RR+NLP and the constant policies achieve, respectively, only 0.7 and 0.59, which means that ACLP outperforms the previously proposed open-loop power adaptation policy by 30% and the non-adaptive power allocation by 52%. We now examine the policies (power-time function) for MDP, RR+NLP and ACLP in Figure 11. For a fair comparison, we have chosen

[5]The reason that we are able to achieve the optimum performance with such a small power allocation is because the nanomotes need to communicate only with their immediate neighbors.

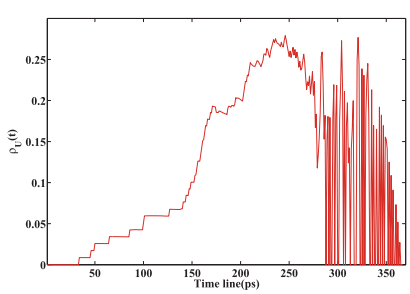

(a) Probability of undesired reaction (HTP) during an uncontrolled FT reactor.

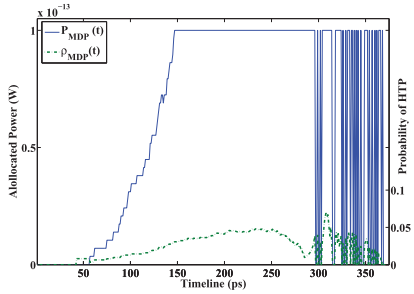

(b) Power allocation via optimal policy, P_{MDP}, and its effect on the probability of undesired reaction, ρ_{MDP}.

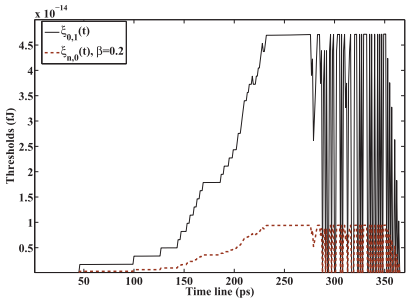

(c) Nanmotes change their receiver thresholds dynamically according to the approximated channel state.

Fig. 9. The performance of MDP in suppressing the rate of undesired reactions.

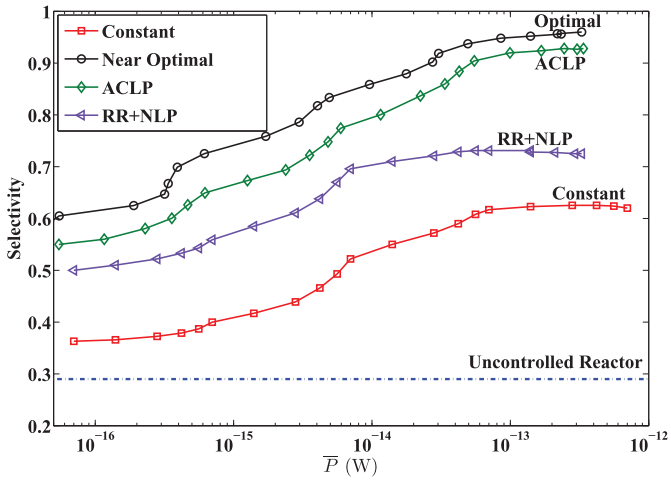

Fig. 10. The selectivity achieved by different power allocation policies for a given power budget.

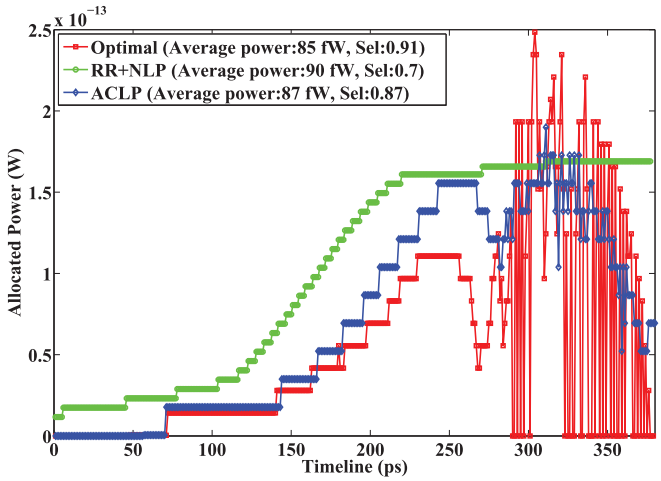

Fig. 11. Typical policies for MDP, RR+NLP and ACLP.

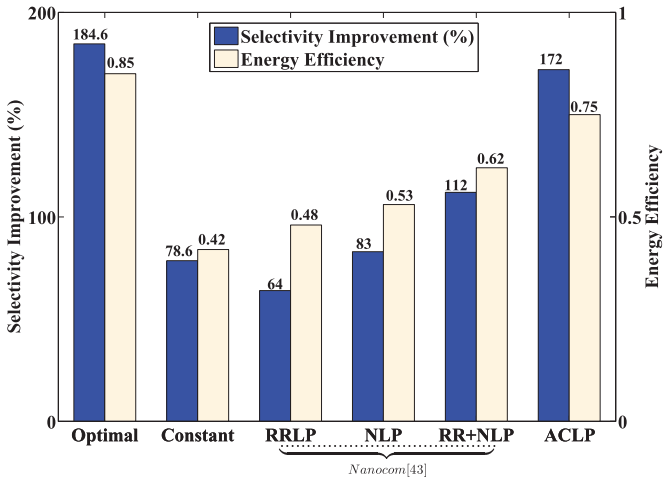

Fig. 12. Average selectivity improvement and average selectivity-to-power ratio for different policies.

three policies which consume around 85fW over one simulation run. The RR+NLP policy achieves a lowest selectivity of 0.7 among the three policies. It places most of its power at where HTP reaction rates or noise is high. MDP achieves a selectivity of 0.91 and allocates an optimized power when the HTP is high. The MDP policy fluctuates between high and low power near the end of the synthesis because of fluctuating HTP reaction rates during the same period of time. The MDP policy therefore smartly switches off the nanomotes when there are no HTP reactions. However, MDP can only achieve that by knowing what the exact chemical composition of the reactor is. The ACLP policy achieves an intermediate selectivity of 0.87. This policy also uses a high power when the HTP reaction rate is high but because it does not know the reactor state, it does not know the exact time to turn off the nanomotes to save power.

The comparison in Figure 11 is for one particular power consumption. We now demonstrate that the relative performance of the four policies, in terms of selectivity and power consumption, holds for different power consumption levels too. We define selectivity improvement of a policy as the percentage improvement using the selectivity of an uncontrolled FT process as the reference. We plotted the average selectivity improvement of MDP, ACLP, RR+NLP and constant power policy in Figure 12. The performance figure is averaged over nominal power levels in the range 10^{-16} to 10^{-12}. MDP achieves an average selectivity improvement of 184.6% while ACLP comes in a close second at 172%, or a 9% performance gap. We hypothesize that this gap is due to difference between $\vec{s}_{\text{AVG}}(t)$ and the actual composition of the channel which was around 12%. We measure the power efficiency of a policy by

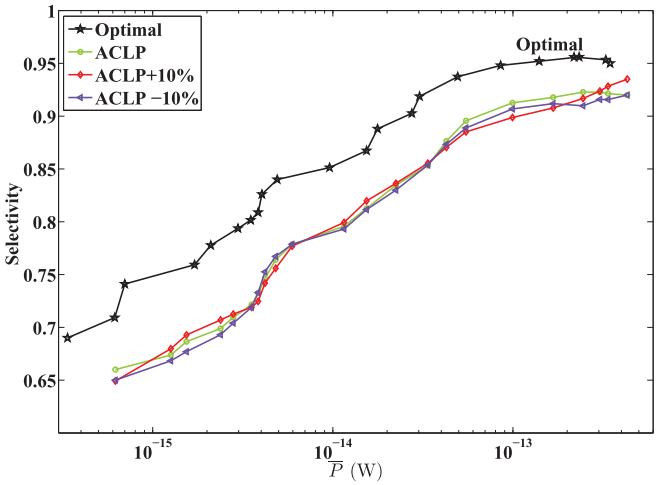

Fig. 13. Selectivity versus power for MDP and ACLP under nominal initial condition, and the two perturbed operating initial conditions.

using the selectivity-to-power ratio. For a given nominal power level P_i and a policy X, we define the selectivity-to-power ratio E_X^i as:

$$E_X^i = \frac{\text{The achieved selectivity using nominal power } P_i}{\text{Average allocated power (fW)}} \quad (15)$$

The selectivity-to-power ratio therefore indicates what selectivity can be achieved by spending a given average power. A higher selectivity-to-power ratio means a more efficient policy. We compute the average selectivity-to-power ratio of the policies by averaging over 20 nominal power levels. The results are shown in Figure 12. It shows the MDP and ACLP have the best average selectivity-to-power ratio at, respectively, 0.85 and 0.75.

We now turn to study the robustness of the local policies. When we design the local policies, we assume that the initial composition (which will be referred to as the nominal initial composition) is given. In the above performance study, we assume that the initial composition of the reactor is the nominal initial composition. However, it may not be possible to control the operating initial composition in a reactor precisely. Here, we study the performance of the local policies when the operating initial composition in the reactor is different from the nominal initial composition. The nominal initial composition used for design is 100 carbon monoxide and 250 hydrogen atoms. In this study, we use two perturbed operating initial compositions: 90 carbon monoxide and 225 hydrogen atoms (-10% deviation) and 110 carbon monoxide and 275 hydrogen atoms ($+10\%$ deviation). We plot the results on selectivity versus power in figure 13 for ACLP. The figure shows the results for MDP, and ACLP under the nominal initial composition, as well as under the two perturbed operating initial compositions. It can be seen from the figure that the performance of ACLP is robust.

Finally, we investigate the performance of ACLP when the small-scale optimal power vector is used to approximate a large-scale process. We consider a large-scale input with the number of CO and H molecules increased by a factor of 1000x compared to the small-scale process with 100 CO molecules and 250 H atoms. This also extends the duration of the FT

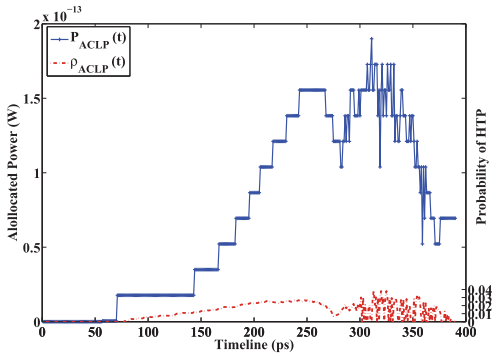

(a) Initial input of CO=100, H=250, $\bar{P} = 71fW$, selectivity=0.85

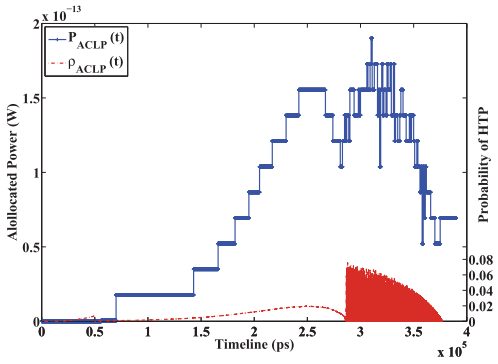

(b) Initial input of CO=100,000, H=250,000, $\bar{P} = 70fW$, selectivity=0.81

Fig. 14. Approximation of P_{ACLP} for a large-scale reactor via a small- scale. Power allocation via ACLP, P_{ACLP} and its effect on the rate of undesired reactions, $\rho ACLP$.

process by 1000 times. Therefore, the optimal power of one time slot in the small-scale process is used to approximate the power allocation of 1000 time slots in the large-scale. That is, in the large-scale, we use the same power for each group of 1000 slots. In other words, the slot sizes are considered 1000 times larger in the large process. The results are shown in Figure 14, which plots the allocated powers and the HTP rates over time for both the small and the large-scale processes. First, we notice a 'stair-case' power allocation for the large-scale, because the same power is allocated for 1000 slots. However, despite this approximation in power allocation, we find that the HTP rates, which are controlled by the allocated powers, have a similar shape and values. Since the selectivity is influenced by the HTP rates, we can expect similar results for the selectivity. Indeed, we find that the resulting selectivity for small-scale and large-scale is, respectively, 0.85 and 0.81. The average power consumed for small-scale and large-scale is, respectively, 71fW and 70fW. These results confirm that even when the ACLP is used to approximate the power allocation for a process 1000x larger than the simulated process, the selectivity and power consumption remains within 5% of the small- scale process.

C. Impact of the Number of Available Power Levels

The earlier results are obtained by assuming m discrete power levels, with $m = 30$, are available for the nanomotes

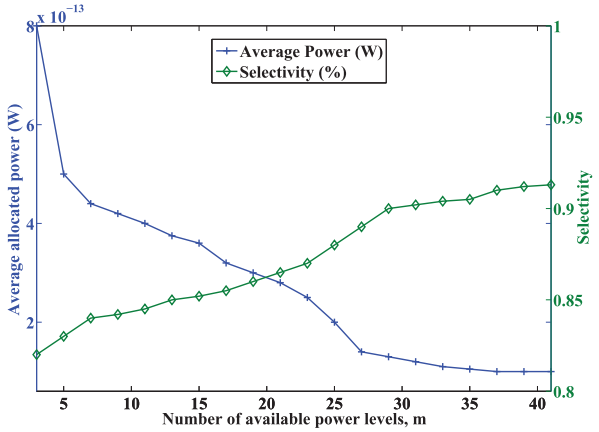

Fig. 15. The impact of the number of available power levels m on selectivity and average power consumption.

to choose from. Given that nanomotes have limited capability, they may only be able to use a small number of power levels. In this section, we investigate the impact of the number of available power levels m on the selectivity and power consumption. We will limit our study to the ACLP because it is the best performing local policy.

We first recall how we generated the m power levels earlier. The lowest power level is $P_1 = 0$, which means the nanomotes do not communicate. The other $m - 1$ power levels are drawn uniformly from $[\frac{P_{\text{nominal}}}{1000}, P_{\text{nominal}}]$ with maximum power $P_m = P_{\text{nominal}}$. We will continue to use this method to generate m different power levels. Note that this method keeps the range of power levels the same but different values of m will provide different granularities of available power levels. We conduct simulations to study the impact of different values of m on selectivity and average power consumption. We vary m from 3 to 41 with an increment of 2. For each value of m, we simulate 10 times and present the average result. The results are plotted in Figure 15. We observe that with increasing m, the selectivity improves but the average power consumption decreases. This is expected because a larger m provides more choices and therefore better selectivity and lower power consumption. It is encouraging to see that the selectivity decreases gracefully with decreasing m. For $m = 41$, the achieved selectivity is 0.913 and for $m = 3$, the selectivity is 0.82, which is still very high.

VII. Discussions

In this section, we briefly discuss the feasibility of the proposed WNSNs that can control a chemical reactor; the possibility of using self-powered WNSN; and the required time to process a query in the proposed protocol in Section III

A. Feasibility and Cost Analysis

The feasibility of realizing such WNSNs are justified by the recent developments in nanoscale catalyst preparation in which species (such as nanomote) could be incorporated at the atomic level [7], [21]. For example, in [7], carbon and nitrogen were co-doped to enhance visible photoactivity of the material. If the optoelectronic property of a catalyst can be improved via nanoscale modification as demonstrated in [7], then a nanomote can be equally atomically integrated since optoelectronic properties are also linked with electromagnetic character. The fact that the method is now routinely done in the laboratory and also with high throughput synthesis means that commercialization is realizable. Additionally, we envision atom-sized nano carbon (graphene) as the nanomote in view of the previous work by Jornet & Akyildiz [3]. Indeed, other components used in the fabrication of the nanomote such as ZnO, are also frequently present in FT catalyst preparation, thus, the nanomote synthesis will be carried out either concurrently with the FT catalyst or post-doped in a subsequent step. Regardless, the nanomote-enhanced FT catalyst preparation is available from current laboratory techniques in catalyst production [8], [10], [49]. A detailed cost-analysis of such production, however, is premature given that pilot-scale manufacturing based on the laboratory methods is still unavailable.

B. Self-Powered WNSNs

We have recently investigated the possibility of using pyroelectric nanogenerators to form a self-powered WNSN within chemical reactors [44], [46]. Basically, when a reaction takes place, energy can be absorbed and released. The heat changes create a temperature gradient which can be harvested by pyroelectric generators. The harvested energy can be stored in a capacitor to power the terahertz wireless transmitter. However, it is possible that the power demanded by the local policies $P(t)$ at time t would be greater than the actual amount of power available at the capacitor. One possible option is to use the available power at the capacitor. A key problem with energy harvesting WNSN therefore is the possibility of allocating an extremely low power if the capacitor level falls drastically. We will investigate the performance our proposed power allocation policies in self-powered WNSNs in future studies.

C. Processing Time

In the proposed neighborhood search protocols in Section III, the required time to process a query plus the time for checking if the site contains a molecule of C_nH_{2n+1} is important. Each nanomote has a flag that is saved in a nanomemory to indicate the existence of C_nH_{2n+1} at its site. Whenever a C_nH_{2n+1} is formed at the site, the flag is set to 1 and when other molecules are formed the flag is set to 0. Therefore, the memory access time is important. The currently available nanoscale memories can read/write a single bit in less than few nanoseconds [28], [38] and this satisfies our application's requirement. Regarding to the processing time, theoretically, the switching frequency of nanoscale transistors such as carbon nanoribbon and carbon nanotube transistors are around 10 THz [25]; this is good enough for our application.

VIII. Conclusions

We have shown that WNSNs operating within a chemical reactor cannot achieve good performance with constant power

allocation due to the time varying terahertz channel caused by chemical composition variation over time. Given the channel state feedback, MDP can be used to optimally adapt the power allocation to maximize reactor selectivity, but channel feedback is difficult to achieve due to computation and communication constraints at the nanoscale. We have proposed an open-loop power adaptation policy that is based on estimating the channel evolution over time using only offline simulations of the reaction process. Using extensive simulations, we have shown that the proposed open-loop policy is capable of achieving near optimal performance without the channel feedback.

REFERENCES

[1] A. Adesina, "Hydrocarbon synthesis via Fischer-Tropsch reaction: Travails and triumphs," *Appl. Catal. A, Gen.*, vol. 138, no. 2, pp. 345–367, 1996.

[2] I. F. Akyildiz, F. Brunetti, and C. Blázquez, "Nanonetworks: A new communication paradigm," *Comput. Netw.*, vol. 52, no. 12, pp. 2260–2279, Aug. 2008.

[3] I. F. Akyildiz and J. M. Jornet, "Electromagnetic wireless nanosensor networks," *Nano Commun. Netw.*, vol. 1, no. 1, pp. 3–19, Mar. 2010.

[4] L. S. Rothman *et al.*, "The HITRAN2012 molecular spectroscopic database," *J. Quant. Spectrosc. Radiat. Transfer*, vol. 130, no. 1, pp. 4–50, Nov. 2013.

[5] N. Buchbinder, L. Lewin-Eytan, I. Menache, J. Naor, and A. Orda, "Dynamic power allocation under arbitrary varying channels: An online approach," *IEEE/ACM Trans. Netw.*, vol. 20, no. 2, pp. 477–487, Apr. 2012.

[6] S. Cui and F. Xiong, "M-ary energy detection of a Gaussian FSK UWB system," *EURASIP J. Wireless Commun. Netw.*, vol. 2014, no. 1, p. 87, 2014.

[7] G. Dai, S. Liu, Y. Liang, H. Liu, and Z. Zhong, "A simple preparation of carbon and nitrogen co-doped nanoscaled TiO2 with exposed 0 0 1 facets for enhanced visible-light photocatalytic activity," *J. Mol. Catal. A, Chem.*, vol. 368–369, pp. 38–42, Mar. 2013.

[8] J. A. Daz *et al.*, "Cobalt and iron supported on carbon nanofibers as catalysts for Fischer–Ttropsch synthesis," *Fuel Process. Technol.*, vol. 128, pp. 417–424, 2014.

[9] C. Falconi, A. Damico, and Z. Wang, "Wireless Joule nanoheaters," *Sens. Actuators*, vol. 127, no. 1, pp. 54–62, Oct. 2007.

[10] T. Fu and Z. Li, "Review of recent development in co-based catalysts supported on carbon materials for Fischer–Tropsch synthesis," *Chem. Eng. Sci.*, vol. 135, pp. 3–20, 2015, SI:TJU 120th anniversary.

[11] M. A. Gibson and J. Bruck, "Efficient exact stochastic simulation of chemical systems with many species and many channels," *J. Phys. Chem. A*, vol. 104, no. 9, pp. 1876–1889, Mar. 2000.

[12] D. Gillespie, "Exact stochastic simulation of coupled chemical reactions," *J. Phys. Chem.*, vol. 81, no. 25, pp. 2340–2361, Dec. 1977.

[13] D. Gillespie, "A rigorous derivation of the chemical master equation," *Phys. A, Stat. Mech. Appl.*, vol. 188, pp. 404–425, Sep. 1992.

[14] C. Intanagonwiwat, R. Govindan, D. Estrin, J. Heidemann, and F. Silva, "Directed diffusion for wireless sensor networking," *IEEE/ACM Trans. Netw.*, vol. 11, no. 1, pp. 2–16, Feb. 2003.

[15] J. Jornet and I. Akyildiz, "Channel modeling and capacity analysis for electromagnetic wireless nanonetworks in the terahertz band," *IEEE Trans. Wireless Commun.*, vol. 10, no. 10, pp. 3211–3221, Oct. 2011.

[16] J. M. Jornet and I. F. Akyildiz, "Channel capacity of electromagnetic nanonetworks in the Terahertz band," in *Proc. IEEE Int. Conf. Commun.*, May 2010, pp. 1–6.

[17] J. M. Jornet and I. F. Akyildiz, "Joint energy harvesting and communication analysis for perpetual wireless nanosensor networks in the terahertz band," *IEEE Trans. Nanotechnol.*, vol. 11, no. 3, pp. 570–580, May 2012.

[18] J. M. Jornet and I. F. Akyildiz, "Femtosecond-long pulse-based modulation for terahertz band communication in nanonetworks," *IEEE Trans. Commun.*, vol. 62, no. 5, pp. 1742–1754, May 2014.

[19] J. M. Jornet and I. F. Akyildiz, "Graphene-based plasmonic nano-transceiver for terahertz band communication," in *Proc. 8th Eur. Conf. Antennas Propag. (EuCAP)*, The Hague, The Netherlands, 2014, pp. 2–6.

[20] M. Kearns, Y. Mansour, and A. Ng, "A sparse sampling algorithm for near-optimal planning in large Markov decision processes," *Mach. Learn.*, vol. 49, pp. 193–208, Dec. 2002.

[21] M. Kolb, W. Maier, and K. Stwe, "High-throughput syntheses of nanoscaled mixed metal sulphides," *Catal. Today*, vol. 159, no. 1, pp. 64–73, 2011, Latest Developments in Combinatorial Catalysis Research and High-Throughput Technologies.

[22] I. Llatser, A. Mestres, S. Abadal, and E. Alarcón, "Time and frequency domain analysis of molecular absorption in short-range terahertz communications," *IEEE Antennas Wireless Propag. Lett.*, vol. 14, pp. 350–353, Feb. 2015.

[23] A. NakhaeiPour, M. R. Housaindokht, S. F. Tayyari, and J. Zarkesh, "Fischer–Tropsch synthesis by nano-structured iron catalyst," *J. Nat. Gas Chem.*, vol. 19, no. 3, pp. 284–292, May 2010.

[24] M. Neely, E. Modiano, and C. Rohrs, "Dynamic power allocation and routing for time-varying wireless networks," *IEEE J. Sel. Areas Commun.*, vol. 23, no. 1, pp. 89–103, Jan. 2005.

[25] Y. Ouyang, Y. Yoon, J. K. Fodor, and J. Guo, "Comparison of performance limits for carbon nanoribbon and carbon nanotube transistors," *Appl. Phys. Lett.*, vol. 89, no. 20, pp. 1–3, 2006.

[26] A. Renken and L. Kiwi-Minsker, "Microstructured catalytic reactors," *Adv. Catal.*, vol. 53, no. 10, pp. 47–122, 2010.

[27] L. Shi, K. Tao, T. Kawabata, T. Shimamura, X. J. Zhang, and N. Tsubaki, "Surface impregnation combustion method to prepare nanostructured metallic catalysts without further reduction: As-burnt Co/SiO2 catalysts for Fischer–Tropsch synthesis," *ACS Catal.*, vol. 1, no. 10, pp. 1225–1233, 2011.

[28] S. Sundaram, P. Elakkumanan, and R. Sridhar, "High speed robust current sense amplifier for nanoscale memories: A winner take all approach," in *Proc. 19th Int. Conf. VLSI Des./5th Int. Conf. Embedded Syst. Des.*, Jan. 2006, p. 6.

[29] L. Tassiulas and A. Ephremides, "Stability properties of constrained queueing systems and scheduling policies for maximum throughput in multihop radio networks," *IEEE Trans. Automat. Control*, vol. 37, no. 12, pp. 1936–1948, Sep. 1992.

[30] G. Thatte and U. Mitra, "Sensor selection and power allocation for distributed estimation in sensor networks: Beyond the star topology," *IEEE Trans. Signal Process.*, vol. 56, no. 7, pp. 2649–2661, Jul. 2008.

[31] G. P. Van Der Laan and A. A. C. M. Beenackers, "Kinetics and selectivity of the Fischer–Tropsch synthesis: A literature review," *Catal. Rev.*, vol. 41, nos. 3–4, pp. 255–318, Jan. 1999.

[32] P. Van Mieghem, *Performance Analysis of Communications Networks and Systems*. Cambridge, U.K: Cambridge Univ. Press, 2009.

[33] J. Villatoro and D. Monzón-Hernández, "Fast detection of hydrogen with nano fiber tapers coated with ultra thin palladium layers," *Opt. Exp.*, vol. 13, no. 13, pp. 5087–5092, Jun. 2005.

[34] F. Vullum and D. Teeters, "Investigation of lithium battery nanoelectrode arrays and their component nanobatteries," *J. Power Sources*, vol. 146, nos. 1–2, pp. 804–808, Aug. 2005.

[35] F. Vullum, D. Teeters, A. Nyten, and J. Thomas, "Characterization of lithium nanobatteries and lithium battery nanoelectrode arrays that benefit from nanostructure and molecular self-assembly," *Solid State Ionics*, vol. 177, nos. 26–32, pp. 2833–2838, Oct. 2006.

[36] Z. L. Wang, "Energy harvesting for self-powered nanosystems," *Nano Res.*, vol. 1, no. 1, pp. 1–8, Jul. 2008.

[37] Y. Yang *et al.*, "Pyroelectric nanogenerators for harvesting thermoelectric energy," *Nano Lett.*, vol. 12, no. 6, pp. 2833–2838, Jun. 2012.

[38] Y. C. Yang, F. Pan, Q. Liu, M. Liu, and F. Zeng, "Fully room-temperature-fabricated nonvolatile resistive memory for ultrafast and high-density memory application," *Nano Lett.*, vol. 9, no. 4, pp. 1636–1643, 2009.

[39] C. R. Yonzon, D. A. Stuart, X. Zhang, and A. D. McFarland, "Towards advanced chemical and biological nanosensors—An overview," *Talanta*, vol. 67, no. 3, pp. 438–448, 2005.

[40] E. Zarepour, A. A. Adesina, M. Hassan, and C. T. Chou, "Nano sensor networks for tailored operation of highly efficient gas-to-liquid fuels catalysts," in *Proc. Australas. Chem. Eng. Conf.*, Brisbane, QLD, Australia, Sep. 29/Oct. 2, 2013, pp. 1–6.

[41] E. Zarepour, A. A. Adesina, M. Hassan, and C. T. Chou, "Innovative approach to improving gas-to-liquid fuel catalysis via nanosensor network modulation," *Ind. Eng. Chem. Res.*, vol. 53, no. 14, pp. 5728–5736, 2014.

[42] E. Zarepour, M. Hassan, C. T. Chou, and A. A. Adesina, "Nanoscale sensor networks for chemical catalysis," in *Proc. IEEE Int. Conf. Nanotechnol.*, Beijing, China, Aug. 5–8, 2013, pp. 61–66.

[43] E. Zarepour, M. Hassan, C. T. Chou, and A. A. Adesina, "Power optimization in nano sensor networks for chemical reactors," in *Proc. ACM Int. Conf. Nanoscale Comput. Commun.*, Atlanta, GA, USA, 2014, pp. 1–9.

[44] E. Zarepour, M. Hassan, C. T. Chou, and A. A. Adesina, "Remote detection of chemical reactions using nanoscale terahertz communication powered by pyroelectric energy harvesting," in *Proc. 2th ACM Int. Conf. Nanoscale Comput. Commun.*, Boston, MA, USA, Sep. 21–22, 2015, pp. 1–6.
[45] E. Zarepour, M. Hassan, C. T. Chou, and A. A. Adesina, "Frequency hopping strategies for improving terahertz sensor network performance over composition varying channels," in *Proc. IEEE Int. Symp. World Wireless Mobile Multimedia Netw. (WoWMoM)*, Sydney, NSW, Australia, Jun. 2014, pp. 1–9.
[46] E. Zarepour, M. Hassan, C. T. Chou, and A. A. Adesina, "Self-powered wireless nano-scale sensor networks within chemical reactors," Sch. Comput. Sci. Eng., Univ. New South Wales, Sydney, NSW, Australia, Tech. Rep. 201423, Oct. 2014.
[47] E. Zarepour, M. Hassan, C. T. Chou, and M. Ebrahimi Warkiani, "Design and analysis of a wireless nanosensor network for monitoring human lung cells," in *Proc. 10th Int. Conf. Body Area Netw. (BodyNets'15)*, Sydney, NSW, Australia, 2015, pp. 1–6.
[48] X. Zhang, H. V. Poor, and M. Chiang, "Optimal power allocation for distributed detection over MIMO channels in wireless sensor networks," *IEEE Trans. Signal Process.*, vol. 56, no. 9, pp. 4124–4140, Sep. 2008.
[49] H. Zhao, Q. Zhu, Y. Gao, P. Zhai, and D. Ma, "Iron oxide nanoparticles supported on pyrolytic graphene oxide as model catalysts for Fischer–Tropsch synthesis," *Appl. Catal. A, Gen.*, vol. 456, pp. 233–239, 2013.

Eisa Zarepour received the Bachelor's degree in computer engineering from the University of Razi, Kermanshah, Iran, in 2003, the Master's degree in software engineering from Sharif University of Technology, Tehran, Iran, in 2006, and the Ph.D. degree in electromagnetic wireless nanoscale sensor network from the University of New South Wales (UNSW), Sydney, N.S.W., Australia, in 2015. He is a Postdoctoral Research Associate with the Networked Systems and Security Group, School of Computer Science and Engineering, UNSW. During his Ph.D. studies, he published 15 peer-reviewed papers and received five awards. His research interests include nanoscale communication, specializing in designing efficient communication protocols for wireless nanoscale sensor networks, mobile data communication, and higher frequency wireless communication and privacy.

Mahbub Hassan received the M.Sc. degree from the University of Victoria, Victoria, BC, Canada, and the Ph.D. degree from Monash University, Melbourne, Vic., Australia, both in computer science. He is a Full Professor with the School of Computer Science and Engineering, University of New South Wales, Sydney, Australia. He was a Visiting Professor at Osaka University, Suita, Japan, University of Nantes, Nantes, France, and National ICT Australia (NICTA). He has coauthored three books, one U.S. patent, and over 150 refereed articles. His research interests include mobile networks, nanoscale wireless sensor network, self-powered and energy-harvesting wireless networks, Internet of Things, and wearable computing. He is a Distinguished Lecturer of IEEE (COMSOC) from 2013 to 2016. He is currently an Editor of the IEEE COMMUNICATIONS SURVEYS AND TUTORIALS and has previously served as a Guest Editor for the IEEE NETWORK and an Associate Technical Editor for the *IEEE Communications Magazine*.

Chun Tung Chou received the B.A. degree in engineering science from the University of Oxford, Oxford, U.K., and the Ph.D. degree in control engineering from the University of Cambridge, Cambridge, U.K. He is an Associate Professor with the School of Computer Science and Engineering, University of New South Wales, Sydney, N.S.W., Australia. He has published over 150 articles on various topics, including, systems and control, wireless networks, and communications. His research interests include molecular communication, nanoscale communication, compressive sensing, and embedded networks.

Adesoji A. Adesina received the Ph.D. degree from the University of Waterloo, Waterloo, ON, Canada, in 1986. He is a Chemical Engineer with over 30 years experience in industry and academia. For over two decades, he was a Professor of chemical engineering with the University of New South Wales, Sydney, N.S.W., Australia, where he established a first-class research facility in catalytic and multiphase reaction engineering. He is currently the founder and CEO of ATODATECH LLC, a private engineering consulting company in California. He has more than 400 refereed publications in catalysis and reaction engineering with focus on energy and environmental technologies. He is a Chartered Engineer and a Fellow of the Institution of Chemical Engineers, U.K.